ILASS-Americas 29th Annual Conference on Liquid Atomization and Spray Systems, Atlanta, GA, May 2017

Spatial-temporal flow dynamics prediction in a large design space via data-driven method

Y.H. Chang, L. Zhang, X.Wang, S.T. Yeh,
S. Mak[†], C.L. Sung[†], C. F. J. Wu[†], V. Yang[*]

School of Aerospace Engineering
Georgia Institute of Technology
Atlanta, Georgia, USA

School of Industrial and Systems Engineering
Georgia Institute of Technology
Atlanta, Georgia, USA[†]

Abstract

This is an interdisciplinary study combining machine-learning techniques, statistics, and physics analyses. To develop a robust propulsion system efficiently, understandings of underlying physics, coupling, and conflicting of the design parameters are significantly important to achieve the optimal design. The large eddy simulation (LES) technique has been widely used to simulate flow physics and combustion characteristics inside rocket engines for decades; however, it consumes great amount of time and resources, which is impractical for design purposes. The purpose of this work is to predict spatial-temporal flowfields using data-driven surrogate model in a short turnaround time. Our previous study has demonstrated a novel design strategy based on the Kernel-smoothed proper orthogonal decomposition (KSPOD) for the swirl injector design. The instantaneous flow dynamics in swirl injectors were well predicted in a small geometry range via kriging based weighting function from design matrix. To further discuss the capability of the emulator for the instantaneous turbulent flow dynamics, the current work extends the design method to a large design space across RD-0110 and RD-170 engines. Overall, the emulator captures most of the flow dynamic details. It also well predicts the performance measures such as the liquid film thickness and the spreading angle. At the same time, the turnaround time for evaluating a new design point is reduced significantly compared with other algorithms and the resultant CPU time is over 2,000 times shorter than that in the LES simulation.

Introduction

The present work extends our previous study that has proposed a data-driven method to predict instantaneous flowfields within a broad geometric range in a short turnaround time. The whole work deals with an interdisciplinary research that has assembled extensive expertise in the computational fluid dynamics (CFD), Design of Experiment (DoE), reduced-basis modeling, statistics, and data-driven analyses.

To design a new propulsion system efficiently, understanding, analyzing, predicting fluid dynamics, and enhancing the interpretation of physical mechanisms for propulsion systems are very important. However, both physical and computational experiments for high-pressure power generation and propulsion systems, such as those of airbreathing and rocket engines [1], are not only challenging [2-4], but also costly and time consuming. Hence, a new methodology to speed up the design process, especially for complex case studies, is required. In our previous study [5], a proper orthogonal decomposition (POD) based kriging model, Kernel-smoothed POD (KSPOD), was proposed and exercised in a small geometry. Kriging is a powerful machine-learning tool for interpolation and prediction which originated from geostatistics studies [6-8]. It models the unknown responses using a Gaussian Process conducted by a preset covariance function. The response surface of the training Kriging model can be evaluated via data-tuned weights to radial basis functions centered at observed points. For an efficient data-reduction process, POD, a well-developed data analysis method, is applied to the emulator. KSPOD can efficiently reduce data generated by high-fidelity simulations to improve the modeling capabilities substantially.

This representative metamodeling technique has substantially improved the modeling capabilities of this approach. As shown in Fig.Figure 1, KSPOD is able to emulate flowfields with detailed turbulent dynamics. The results are not only qualitatively accurate, but also exhibit extraordinary quantitative capabilities to predict performance measurements (e.g. liquid film thickness and spreading angle) and dominant POD frequencies. Lastly, the emulation can be done in an extremely short turnaround time which is over 4,000 times faster than a high-fidelity simulation.

Although KSPOD has brought some promising breakthroughs, the whole work was practiced under a small design space [5]. To further examine the capability and reliability of this method, a broad range of design space must be applied. In this work, the CFD datasets are same as those applied in a previous study for Common-grid POD (CPOD) [11], which predicted mean flowfields very well. Liquid film thickness and spreading angle are two indicators frequently used to evaluate the performance of injectors [9, 10]. Those previous studies have provided prior knowledge of the major contributing geometric parameters [10, 11]. They have shown that the size of injection slit, location of slit, and the intake angle are the three parameters that have the greatest influences on the liquid film thickness and spreading angle. The current work aims to apply KSPOD to the instantaneous flowfield predictions over a broad range of geometric parameters.

The paper is structured as follows: methodology, including the baseline swirl injector configuration, sample points designated by the DoE, the CFD framework, and algorithm of the emulation model; results and discussion focus on the comparison between simulation and emulation results with quantitative analyses; and conclusions with directions for future work.

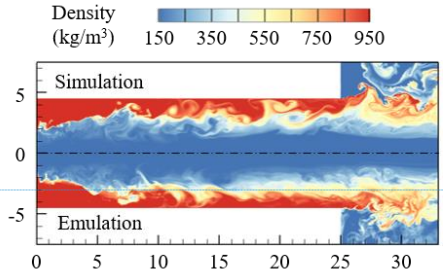

Figure 1. Comparison of instantaneous density distribution at t = 3 ms.

Methodology

1. Baseline swirl injector configuration

Figure 2 shows a schematic of a swirl injector typically used in liquid-propellant rocket engines. The five variables that define the geometry are injector length, L, nozzle radius, R_n, injection slit width, δ, injection angle, θ, and the distance between the slit and headend, ΔL. These geometric parameters play important roles in determining the injector performance, such as liquid film thickness, h and spreading angle, α. The former controls the size of fluid particle for atomization and the latter affects mixing efficiency. The selection of these design variables is dependent upon the engine requirements. To generalize the current framework, a broad span of these variables was decided. Table 1 shows flow conditions in CFD works. Table 2 tabulates the design variables and their ranges. It also lists a set of design to validate the accuracy of surrogate model (i.e. emulator). The injector length spans the lengths for flight-proven engines, which are about 22.7 and 93 mm for the RD-0110 and RD-170 engine, respectively. The two baseline design models were chosen because of their good reputations and huge geometric differences.

The swirl injector in Figure 2 burns liquid oxygen (LOX) and kerosene in a gas generator combustion system; however, this study focus on cold flow and

Commented [LZ1]: Reference?

Commented [LZ2]: This sentence needs to be reorganized

Commented [LZ3]: I feel it is better to put this sentence in the first paragraph.

Commented [LZ4]: This sentence needs to be adjusted to better summarize the merits of KSPOD.

Commented [LZ5]: Measurements or measures (I vote for the first)? Please be consistent in the paper.

Commented [LZ6]: Can you make this remark at the beginning of the paper?

Commented [LZ7]: Is this information necessary?

Figure 2 only illustrates the upstream region with LOX mixing with ambient air. Liquid propellant is tangentially introduced into the center post, and develops a thin liquid film that attaches to the wall due to the swirl-induced centrifugal force. Because of conservation of angular momentum, a low-density, hollow gas core forms in the center region. The liquid film exits the injector as a thin conical sheet and subsequently undergoes the atomization process. This type of injector design is prominent in Russian rocket engines and has been employed since the 1970s, such as the third stage of the Soyuz. Flow dynamics in these devices under supercritical conditions have been extensively studied using CFD [10, 12].

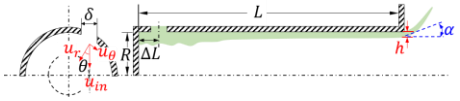

Figure 2. Schematic of baseline injector configuration

Table 1. Flow conditions

T_{in} (K)	T_∞ (K)	$\dot{m}$(kg/s)	P_∞ (MPa)
120	300	0.15	10

Table 2. Design space

Design Variable	Design Range	Validation Case
L	20-100 mm	22 mm
R	2-5 mm	3.22 mm
θ	45°-75°	58.2°
δ	0.5-2 mm	0.576 mm
ΔL	1-4 mm	3.42 mm

2. Design of Experiment (DoE)

The DoE methodology is a statistical approach to building and assessing models through careful selection of input variables for a given design space. As previously mentioned, the number of simulations is usually dependent upon the number of design variables. Due to the expensive computational cost of LES simulations, 30 sets of injector geometries were carefully chosen according to Maximum Projection (MaxPro) design [13]. This number falls within the 5-10 simulation per design variable as suggested in Santner et [14]. For a complex spatiotemporal data set, it would suggest more runs instead of the rules-of-thumb. Different from the popularly used Latin hypercube-based designs [15, 16], MaxPro design possess good space-filling properties on any subspace of the design variables. This projective property allows for accurate predictions from the GP model even when variables have varying levels of importance. A 2D projection of the design points is plotted in Figure 3. The space-filling properties of the DoE are confirmed visually with this projection plot. Each simulation takes about 6 to 7 days parallelized around 200 CPU cores to accumulate statistically significant data with a time span of 30 ms after reaching a fully developed state (~24 ms). The simulated data are subsampled every 30 iteration steps with the time step of 1 μs. According to the Nyquist criterion, a temporal resolution of 16.5 kHz is achieved.

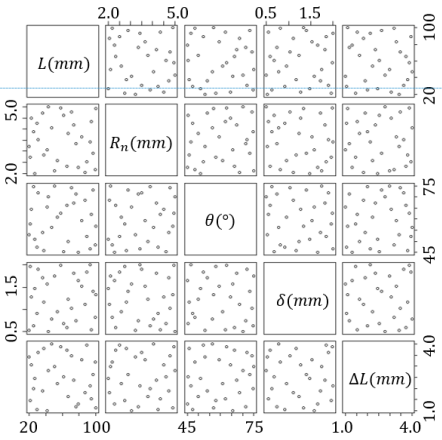

Figure 3. 2D projections of sample points within design space

3. CFD Framework

The theoretical basis of the present high-fidelity simulation is described in Oefelein and Yang [17]. It copes with supercritical fluid flow and combustion over the entire range of fluid thermodynamic states of concern. Turbulent closure is approached by the application of LES technique. The subgrid-scale motions are represented by the Smagorinsky eddy viscosity model proposed by Erlebacher et al. [18]. Density, enthalpy, and specific heat at constant pressure, are evaluated according to the modified Soave-Redlich-Kwong (SRK) equation of state (EOS) and fundamental thermodynamic theories. SRK EOS is used here for its validity over a broad range of fluid states and easy implementation. The Takahashi method calibrated for high-pressure conditions [19] is employed to acquire mass diffusivity. The thermodynamic and transport properties, including thermal conductivity and dynamic viscosity, are estimated according to an extended corresponding-state principle that have been validated and implemented in previous studies [20-23].

The numerical framework is built by conducting a preconditioning scheme and a unified treatment of general-fluid thermodynamics [24]. It applies a density-based, finite-volume methodology, along with a dual-time-step integration technique [25]. A second-order

Commented [LZ8]: Is this information necessary?

backward difference is used to accomplish temporal discretization; and a four-step Runge-Kutta scheme is applied to integrate the inner-loop pseudo-time term. A fourth-order central difference scheme in generalized coordinates is used to obtain spatial discretization. Fourth-order matrix dissipation is taken to assure numerical stability and minimum contamination of the solution developed by Swanson and Turkel [26]. Lastly, a multi-block domain decomposition technique associated with the message passing interface technique of parallel computing is applied to optimize computation speed.

4. Kernel-smoothed POD (KSPOD)

This section introduces KSPOD, a combination of statistical modeling and data-reduction algorithm to obtain a reduced-basis model. Comparing with CFD simulation, this model gives a pragmatic computational turnaround time to obtain large-scale spatiotemporal datasets with new designs.

The statistical modeling and data-reduction are achieved via kriging and POD. Kriging is a method of interpolation that models the interpolated values by a Gaussian process conducted by prior co-variances to optimize smoothness of the fitted values. Traditionally, kriging algorithm has to be applied for each single point. There are over 100,000 grid points in each simulation and using kriging over every single point would be impractical. The solution is to conduct kriging with the aforementioned data-reduction method, POD.

The idea of POD yields eigen-functions and their corresponding coefficients, i.e. POD modes and coefficients. These POD modes represent the important flow physics involved in flowfields. For a given flow property, the POD analysis determines a set of orthogonal basis functions. The optimal basis functions (i.e. POD modes) are formed by introducing an inner product for an eigen-decomposition [27-29]. The basis functions are essentially spatial distributions of the fluctuation field of the flow response including but not limited to pressure, density, temperature, and velocity components; and they represent dominant coherent structures with meaningful physical interpretation, such as the acoustic energy of the oscillatory field [30]. A spectral analysis with POD coefficients can be conducted to identify the flow periodicity and characteristic frequencies for the extracted physics, such as hydrodynamic and acoustic instabilities [10]. The rank of POD mode is determined by the corresponding eigenvalue, which is proportional to the inner product of snapshot component of interest.

Notwithstanding the limited number of training points within the described design space, it is imperative to apply POD while tuning the emulation model. The decomposition process accomplishes significant data reduction while containing principle physical information of flowfield from the complex nature of the simulation results. Since POD simplifies the total information from spatial-temporal flowfield, a kriging based model can be applied to tune a surrogate emulator over POD modes and coefficients for prediction.

In KSPOD, all cases have to be processed POD individually before model training. There are two implicit assumptions for KSPO. The first assumption is, for similar geometric designs, the physics extracted by POD modes in different cases shall be alike under the same rank of order. The second assumption is that the dominant modes capturing similar physics should be transferred with the same or similar phase. It means that those physics will be reserved and taken care by kriging, a Bayesian spatial function, to generate a weighted average (i.e. posterior result) based on a new design as prediction.

Consider the kriging of the indicator vector $\boldsymbol{e}_i$, for some $i = 1, \cdots n$ where an n-vector with one in the i-th entry, and zero elsewhere. There's another vector $\boldsymbol{r}_i$ where $i = 1, \cdots, p$ and a p-vector denoting the p control settings for design case i. Since a space-filling design is employed, it is easy to show that the optimal correlation parameters for the underlying GP should be equal for all p dimensions. Denote this common correlation as θ. When the number of design points $n \to \infty$, one can similarly show that $\theta \to \infty$ as well, since the "kriging surface" for $\boldsymbol{e}_i$ converges pointwise to a discontinuous surface with value 1 at $\boldsymbol{r}_i$ and 0 elsewhere.

The "kriging" estimate of $\boldsymbol{e}_i$ for a new design setting $\boldsymbol{r}_{new}$ is:

$$\widehat{w}_{\mathrm{new},i} = \hat{\mu} + \boldsymbol{r}_{new}^T \boldsymbol{R}^{-1}(\boldsymbol{e}_i - \hat{\mu}\mathbf{1}_n) \tag{1}$$

, where $\hat{\mu} = (\mathbf{1}_n^T \boldsymbol{R}^{-1}\mathbf{1}_n)^{-1}\mathbf{1}_n^T \boldsymbol{R}^{-1}\boldsymbol{e}_i = \boldsymbol{R}_{ii}^{-1} / \sum_{i=1}^n \boldsymbol{R}_{ii}^{-1}$, $\boldsymbol{R}$ is correlation matrix, and $\widehat{w}_{new,i}$ is a weighted number based on kriging. It is easy to show that, when $\theta \to \infty$ and $n \to \infty$, the best linear unbiased prediction (BLUP) estimator makes $\hat{\mu} \to 0$. Moreover, when $\theta \to \infty$, the inverse correlation matrix $\boldsymbol{R}^{-1}$ converges element-wise to $\mathbf{I}_n$. Under these two approximations, we get:

$$\begin{aligned} \widehat{w}_{new,i} &\approx \boldsymbol{r}_{new}^T \boldsymbol{R}^{-1}\boldsymbol{e}_i \approx \boldsymbol{r}_{new}^T \boldsymbol{e}_i \\ &= \exp\left\{-\theta \left|\left|\boldsymbol{c}_i - \boldsymbol{c}_{new}\right|\right|_2^2\right\} \end{aligned} \tag{2}$$

where $||\cdot||_2$ is the Euclidean norm. In other words, $\widehat{w}_{new,i}$ is simply the isotropic Gaussian kernel $k_\theta(\boldsymbol{c}_i, \boldsymbol{c}_{new})$. The proposed predictor of the k-th mode at new design setting $\boldsymbol{c}_{new}$ is:

$$\hat{\phi}_{new}^k(\boldsymbol{x}) = \frac{\sum_{i=1}^n \widehat{w}_{new,i}\phi_i^k(\boldsymbol{x})}{\sum_{i=1}^n \widehat{w}_{new,i}} \approx \frac{\sum_{i=1}^n k_\theta(\boldsymbol{c}_i, \boldsymbol{c}_{new})\phi_i^k(\boldsymbol{x})}{\sum_{i=1}^n k_\theta(\boldsymbol{c}_i, \boldsymbol{c}_{new})} \tag{3}$$

where $\phi_i^k(\boldsymbol{x})$, $i = 1, \cdots, n$ – The k-th POD mode at design setting $\boldsymbol{c}_i$.

The last expression can be seen to be a kernel smoother on the observed modes $\{\phi_i^k(\boldsymbol{x})\}_{i=1}^n$. Because of this, the method is termed as kernel-smoothed POD technique than kriging, especially the latter leverages different correlation parameters over each dimension to approximate an unknown surface. Here kriging would not apply weighting number $\hat{w}_{new,i}$ to flow field directly. The reason is that the unstable flowfield is a combination of waves with different frequencies, amplitudes, and phases. Simulation cannot control the starting phase for each wave. If the weighting number is used for flow field directly, it is possible that two training data cancel each other during kriging, which means some flow information will be eliminated. The phase difference can be observed in POD modes as well. Applying weighting function to POD modes with kernel-smoothed algorithm can avoid the phase neutralization and retain important physics information.

Once the emulator model is trained, it can be used to predict the flow evolution at a new design point. The computation cost is reduced by around 3 orders of magnitudes. Simulation data took around 7 days with around 200 CPU cores, i.e. approximately 33, 600 CPU hours on average. After training model with sufficient samples, a new flowfield can be evaluated within one minute. Including data loading and saving, the whole process takes 1.5 hours within 10 CPU cores that is 2,240 times faster than simulation.

Results and Discussion

Figure 4 shows the instantaneous density and temperature distributions for the validation case listed in Table 2. The emulation captures the accumulation of liquid propellant at the injector headend, performing better in the upstream section compared to the downstream section. In Figure 4(a), the downstream liquid film thickness and spreading angle are well predicted. The shapes of traveling vortices in the liquid film are also captured by emulation. Similar results for temperature are also captured and illustrated in Figure 4(b). Overall, the shape of liquid film and flowfield distributions are well evaluated by emulation. However, the very detailed structures of the traveling vortices are still missing in emulation. The main reason is the design variables are chosen in a broad range that brings significant influences of the flow dynamics inside the injector.

The emulator is able to predict a liquid film thickness (h) of 0.490 mm and a spreading angle (α) of 50.7° at the injector exit. The actual CFD simulation for this case has a liquid film thickness of 0.430 mm and a spreading angle of 51.6°. At the injector exit, the extracted scalar prediction results achieve a 14% percentage for the liquid film thickness and a 3% percentage error for the spreading angle. The variation of the thickness along the axial distance is shown in Figure 5. It shall be noted that this analysis is based on an inviscid and incompressible analysis. The average error along the axial distance for the liquid film is 6.7%.

In Yeh et. al (2017) [11], the sensitivity analysis revealed that the three most significant design parameters (i.e. L, ΔL, and δ), aspect ratio between L and R, and a broad design space can cause two different flow behaviors in a swirl injector. In the 30 training cases, there are 19 swirl-like and 11 jet-like flows. The flow behavior in validation case is swirl-like. To improve the emulation qualitatively and performance measurement accuracy quantitatively in a broad design space, more design sample cases are needed to enrich physics inside the training data vault.

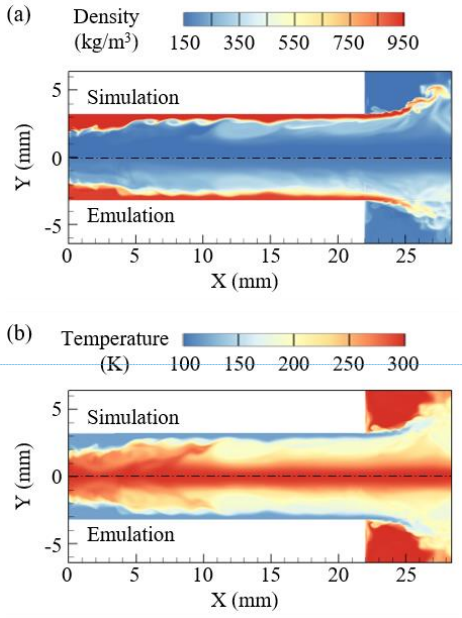

Figure 4. Comparison of instantaneous (a) density and (b) temperature distributions at t = 3 ms.

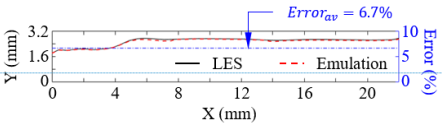

Figure 5. Comparison of mean liquid film thickness and total along axial distance for validation case. The results are averaged over 1000 snapshots.

In summary, KSPOD can be applied in a broad geometry range to provide reasonable prediction for spatiotemporal flowfields. The analyses of performance

Commented [LZ9]: Is it possible to make this part a little longer? Maybe more validation case(s) with a very different set of geometric parameters.

Commented [LZ10]: Is it related to the two assumptions of the KSPOD?

Commented [LZ11]: Which case? What are the conditions for "this case"?

Commented [LZ12]: Need to be edited.

measurements shows quantitatively comparable results. If DoE process provides more sample points, it is highly possible for KSPOD to provide emulated flowfields with high-fidelity qualities. Moreover, this method brings a pragmatic computational turnaround time, which can be further applied for complex case studies for optimal design decision.

Conclusion

Taking a swirl injector as an example, axisymmetric calculations have been performed through the described numerical implementation, which is capable of simulating supercritical fluid injection with mixing and chemically reacting flows over a broad range of fluid thermodynamic states. The main contribution of this work is the incorporation of statistical and machine learning techniques with physics-guided model assumptions to build an efficient surrogate model for flowfield prediction. Additionally, this model can be applied in a broad geometry range for spatiotemporal flow prediction. A vital model assumption is that the KSPOD accurately retains the rich set of physics over varying geometries. This model successfully reproduces the LES results and fared better than the analytical estimation of the performance measures, such as liquid film thickness and spreading angle. Moreover, this methodology significantly reduces the computational time required for surveying the design space for instantaneous extractions. The turnaround time for one emulation case is over 2,000 times shorter. While the focus of the present paper is on the data-driven analysis and emulation of a swirl injector, the principle of applying machine learning techniques with physics-guided assumptions is valuable when considering any spatiotemporal system. For future work, further investigation is needed in dynamic regions of flowfield, where the surrogate model had higher predictive uncertainties. Another potential topic is to extend this idea for more extreme ranges of the design points to predict reacting flowfields.

Nomenclature

$\dot{m}$	mass flow rate
h	liquid film thickness
L	length
t	time
P	pressure
R	radius
T	temperature
α	spreading angle
δ	slit size
θ	intake angle

Subscripts

in	intake
∞	ambient
av	average
em	emulation
si	simulation
θ	tangential
r	radial

References

1. Yang, V., *Modeling of supercritical vaporization, mixing, and combustion processes in liquid-fueled propulsion systems.* Proceedings of the Combustion Institute, 2000. **28**(1): p. 925-942.
2. Mayer, W. and H. Tamura, Propellant injection in a liquid oxygen/gaseous hydrogen rocket engine. Journal of Propulsion and Power, 1996. 12(6): p. 1137-1147.
3. Candel, S., et al., Experimental Investigation of Shear Coaxial Cryogenic Jet Flames. Journal of Propulsion and Power, 1998. 14(5): p. 826-834.
4. Candel*, S., et al., Structure and Dynamics of Cryogenic Flames at Supercritical Pressure. Combustion Science and Technology, 2006. 178(1-3): p. 161-192.
5. Yu-Hung Chang, Liwei Zhang, Shiang-Ting Yeh, Xingjian Wang,Simon Mak, Chih-Li Sung, C. F. J. Wu, Vigor Yang, Highly efficient spatiotemporal flow dynamics prediction via data-driven analysis and LES-based surrogate model Journal of Computational Physics, 2017.
6. Krige, D., A statistical approach to some mine valuations and allied problems at the Witwatersrand. 1951. University of Witwatersrand.
7. Cressie, N., The origins of kriging. Mathematical geology, 1990. 22(3): p. 239-252.
8. Matheron, G., Principles of geostatistics. Economic geology, 1963. 58(8): p. 1246-1266.
9. Zong, N., et al., A numerical study of cryogenic fluid injection and mixing under supercritical conditions. Physics of Fluids, 2004. 16(12): p. 4248-4261.
10. Zong, N. and V. Yang, Cryogenic fluid dynamics of pressure swirl injectors at supercritical conditions. Physics of Fluids, 2008. 20(5): p. 056103.
11. Shiang-Ting Yeh, Xingjian Wang., Chih-Li Sung,Yu-Hung Chang, Simon Mak, C. F. Jeff Wu, Vigor Yang, Data-Driven Analysis and Mean Flow Prediction using a Physics-Based Surrogate Model for Design Exploration. Journal of Computational Physics, 2017.
12. Wang, X., Huo, H., Wang, Y., and Yang, V., A Comprehensive Study of Cryogenic Fluid Dynamics of Swirl Injectors at Supercritical Conditions. AIAA Journal, 2016.
13. Joseph, V.R., E. Gul, and S. Ba, Maximum projection designs for computer experiments. Biometrika, 2015. 102(2): p. 371-380.

Commented [LZ15]: Double check the format. Some author names are incomplete.

Commented [LZ13]: This information is not necessary. I'd prefer a brief summary of the physical problem, and statistic models etc.

Commented [LZ14]: This sentence is hard to understand.

14. Santner, T.J., B.J. Williams, and W.I. Notz, The design and analysis of computer experiments. 2013: Springer Science & Business Media.
15. McKay, M.D., R.J. Beckman, and W.J. Conover, A comparison of three methods for selecting values of input variables in the analysis of output from a computer code. Technometrics, 2000. 42(1): p. 55-61.
16. Morris, M.D. and T.J. Mitchell, Exploratory designs for computational experiments. Journal of statistical planning and inference, 1995. 43(3): p. 381-402.
17. Oefelein, J.C. and V. Yang, Modeling High-Pressure Mixing and Combustion Processes in Liquid Rocket Engines. Journal of Propulsion and Power, 1998. 14(5): p. 843-857.
18. Erlebacher, G., et al., Toward the large-eddy simulation of compressible turbulent flows. Journal of fluid mechanics, 1992. 238: p. 155-185.
19. Takahashi, S., Preparation of a generalized chart for the diffusion coefficients of gases at high pressures. Journal of Chemical Engineering of Japan, 1975. 7(6): p. 417-420.
20. Zong, N., et al., A Numerical Study of Cryogenic Fluid Injection and Mixing under Supercritical Conditions. Physics of Fluids, 2004. 16(12): p. 4248-4261.
21. Wang, X., H. Huo, and V. Yang. Supercritical combustion of general fluids in laminar counterflows. in 51st AIAA Aerospace Sciences Meeting including the New Horizons Forum and Aerospace Exposition. 2013.
22. Huo, H., X. Wang, and V. Yang, A general study of counterflow diffusion flames at subcritical and supercritical conditions: Oxygen/hydrogen mixtures. Combustion and Flame, 2014. 161(12): p. 3040-3050.
23. Wang, X., H. Huo, and V. Yang, Counterflow Diffusion Flames of Oxygen and N-Alkane Hydrocarbons (CH4-C16H34) at Subcritical and Supercritical Conditions. Combustion Science and Technology, 2015. 187(1-2): p. 60-82.
24. Meng, H. and V. Yang, A unified treatment of general fluid thermodynamics and its application to a preconditioning scheme. Journal of Computational Physics, 2003. 189(1): p. 277-304.
25. Hsieh, S.-Y. and V. Yang, A preconditioned flux-differencing scheme for chemically reacting flows at all Mach numbers. International Journal of Computational Fluid Dynamics, 1997. 8(1): p. 31-49.
26. Swanson, R.C. and E. Turkel, On central-difference and upwind schemes. Journal of computational physics, 1992. 101(2): p. 292-306.
27. Berkooz, G., P. Holmes, and J.L. Lumley, The proper orthogonal decomposition in the analysis of turbulent flows. Annual review of fluid mechanics, 1993. 25(1): p. 539-575.
28. Kerschen, G. and J.-C. Golinval, *Physical interpretation of the proper orthogonal modes using the singular value decomposition.* Journal of Sound and Vibration, 2002. **249**(5): p. 849-865.
29. Rowley, C.W., *Model reduction for fluids, using balanced proper orthogonal decomposition.* International Journal of Bifurcation and Chaos, 2005. **15**(03): p. 997-1013.
30. Huang, Y., S. Wang, and V. Yang, *Systematic analysis of lean-premixed swirl-stabilized combustion.* AIAA journal, 2006. **44**(4): p. 724-740.